Chinese Journal of Natural Medicines

Shengmaisan combined with Liuwei Dihuang Decoction alleviates chronic intermittent hypoxia–induced cognitive impairment by activating the EPO/EPOR/JAK2 signaling pathway

Jianchao SI, Xue CHEN, Kerong QI, Dongli LI, Bingbing LIU, Yuying ZHENG, Ensheng JI, Shengchang YANG

Citation: Jianchao SI, Xue CHEN, Kerong QI, Dongli LI, Bingbing LIU, Yuying ZHENG, Ensheng JI, Shengchang YANG, Shengmaisan combined with Liuwei Dihuang Decoction alleviates chronic intermittent hypoxia–induced cognitive impairment by activating the EPO/EPOR/JAK2 signaling pathway, Chinese Journal of Natural Medicines, 2024, 22(5), 426–440. doi: 10.1016/S1875–5364(24)60640–0.

View online: https://doi.org/10.1016/S1875–5364(24)60640–0

Related articles that may interest you

Potentilla anserina polysaccharide alleviates cadmium–induced oxidative stress and apoptosis of H9c2 cells by regulating the MG53–mediated RISK pathway

Chinese Journal of Natural Medicines. 2023, 21(4), 279–291 https://doi.org/10.1016/S1875–5364(23)60436–4

Five Rutaceae family ethanol extracts alleviate H_2O_2 and LPS–induced inflammation *via* NF–κB and JAK–STAT3 pathway in HaCaT cells

Chinese Journal of Natural Medicines. 2022, 20(12), 937–947 https://doi.org/10.1016/S1875–5364(22)60217–6

Dandelion polyphenols protect against acetaminophen–induced hepatotoxicity in mice *via* activation of the Nrf–2/HO–1 pathway and inhibition of the JNK signaling pathway

Chinese Journal of Natural Medicines. 2020, 18(2), 103–113 https://doi.org/10.1016/S1875–5364(20)30011–X

Centranthera grandiflore alleviates alcohol–induced oxidative stress and cell apoptosis

Chinese Journal of Natural Medicines. 2022, 20(8), 572–579 https://doi.org/10.1016/S1875–5364(22)60181–X

Antidepressant–like effects of albiflorin involved the NO signaling pathway in rats model of chronic restraint stress

Chinese Journal of Natural Medicines. 2020, 18(11), 872–880 https://doi.org/10.1016/S1875–5364(20)60030–9

Protective effects of Wuwei Xiaodu Drink against chronic osteomyelitis through $Foxp3^+CD25^+CD4^+$ Treg cells *via* the IL–2/STAT5 signaling pathway

Chinese Journal of Natural Medicines. 2022, 20(3), 185–193 https://doi.org/10.1016/S1875–5364(22)60146–8

Wechat

Available online at www.sciencedirect.com
ScienceDirect
Chinese Journal of Natural Medicines 2024, **22**(5): 426-440
doi: 10.1016/S1875-5364(24)60640-0
Chinese Journal of Natural Medicines

•Original article•

Shengmaisan combined with Liuwei Dihuang Decoction alleviates chronic intermittent hypoxia-induced cognitive impairment by activating the EPO/EPOR/JAK2 signaling pathway

SI Jianchao[1Δ], CHEN Xue[1Δ], QI Kerong[1], LI Dongli[1], LIU Bingbing[1], ZHENG Yuying[1, 3], JI Ensheng[1, 2*], YANG Shengchang[1, 2*]

[1] *Department of Physiology, Hebei University of Chinese Medicine, Shijiazhuang 050000, China;*
[2] *Hebei Technology Innovation Center of TCM Combined Hydrogen Medicine, Shijiazhuang 050000, China;*
[3] *Department of Geriatrics, First People's Hospital of Xiaogan, Xiaogan 432000, China*

Available online 20 May, 2024

[ABSTRACT] Chronic intermittent hypoxia (CIH), a principal pathophysiological aspect of obstructive sleep apnea (OSA), is associated with cognitive deficits. Clinical evidence suggests that a combination of Shengmaisan and Liuwei Dihuang Decoctions (SMS-LD) can enhance cognitive function by nourishing yin and strengthening the kidneys. This study aimed to assess the efficacy and underlying mechanisms of SMS-LD in addressing cognitive impairments induced by CIH. We exposed C57BL/6N mice to CIH for five weeks (20%−5% O_2, 5 min/cycle, 8 h/day) and administered SMS-LD intragastrically (15.0 or 30 g·kg^{-1}·day) 30 min before each CIH session. Additionally, AG490, a JJanus kinase 2 (JAK2) inhibitor, was administered *via* intracerebroventricular injection. Cognitive function was evaluated using the Morris water maze, while synaptic and mitochondrial structures were examined by transmission electron microscopy. Oxidative stress levels were determined using DHE staining, and the activation of the erythropoietin (ER)/ER receptor (EPOR)/JAK2 signaling pathway was analyzed through immunohistochemistry and Western blotting. To further investigate molecular mechanisms, HT22 cells were treated in vitro with either SMS-LD medicated serum alone or in combination with AG490 and then exposed to CIH for 48 h. Our results indicate that SMS-LD significantly mitigated CIH-induced cognitive impairments in mice. Specifically, SMS-LD treatment enhanced dendritic spine density, ameliorated mitochondrial dysfunction, reduced oxidative stress, and activated the EPO/EPOR/JAK2 signaling pathway. Conversely, AG490 negated SMS-LD's neuroprotective and cognitive improvement effects under CIH conditions. These findings suggest that SMS-LD's beneficial impact on cognitive impairment and synaptic and mitochondrial integrity under CIH conditions may predominantly be attributed to the activation of the EPO/EPOR/JAK2 signaling pathway.

[KEY WORDS] Chronic intermittent hypoxia; Cognitive impairment; Shengmaisan; Liuwei Dihuang Decoction; Oxidative stress; EPO/EPOR/JAK2 signaling pathway

[CLC Number] R965 **[Document code]** A **[Article ID]** 2095-6975(2024)05-0426-15

Introduction

Obstructive sleep apnea (OSA) is characterized by the repeated collapse and obstruction of the upper airway during sleep, leading to symptoms such as snoring, sleep fragmentation, daytime fatigue, and drowsiness [1]. In recent years, OSA has garnered significant attention due to its high prevalence and the severity of its associated complications. However, the mechanisms underlying the multi-organ damage observed in patients with OSA remain largely elusive. Chronic intermittent hypoxia (CIH), a key pathological feature of OSA, exerts profound effects on multiple organs, particularly the brain [2]. Cognitive dysfunction represents a frequent complication among OSA patients [3]. The structural alterations in the brain, induced by recurrent episodes of intermittent hypoxia (IH), have been linked to cognitive deficits. These changes include oxidative stress, modifications in synaptic structures, and mitochondrial damage, all of which are believed to contribute to

[Received on] 20-Dec.-2023
[Research funding] This work was supported by the National Natural Science Foundation of China (No. 82274617), the Hebei Natural Science Foundation (Nos. H2022423352, H2022423370), the Fundamental Research Funds for the Provisional Universities of Hebei University of Chinese Medicine (No. YXTD2021005), Yanzhao Medical Research Project of Hebei University of Chinese Medicine (No. YZZY2022004), the Graduate Innovation Fund of Hebei University of Chinese Medicine (No. XCXZZSS2021005).
[*Corresponding author] E-mails: jesphy@126.com (JI Ensheng); yscdekaoyan@163.com (YANG Shengchang)
[Δ]These authors contributed equally to this work.
These authors have no conflict of interest to declare.

the cognitive impairments observed in these patients [4, 5].

According to the kidney-marrow-brain theory in Traditional Chinese Medicine (TCM), the essence of the kidneys is vital for nourishing the muscles and bones and is intimately linked with brain health. This connection between the kidneys and the brain is referred to as "brain-kidney cross-talk" in contemporary medical literature [6, 7]. Kidney-yin deficiency leads to cognitive impairment, and tonifying the kidneys has been performed for treating cognitive impairment in TCM. Previous results have indicated that CIH-exposed mice clinically manifest a "deficiency of both qi and yin" syndrome (DQYS) [8].

DQYS, or "deficiency of both qi and yin" syndrome, is recognized as a prevalent clinical syndrome [9] and is observed in the advanced stages of various acute febrile diseases and numerous chronic conditions characterized by internal damage. Symptoms commonly associated with DQYS include a thin physique, loss of appetite, fatigue, irritability, palpitations, and a fine pulse [10]. Clinical studies have demonstrated that Shengmaisan exhibits significant therapeutic benefits for a range of diseases characterized by DQYS, including pneumonia induced by COVID-19 [11-13]. Moreover, Liuwei Dihuang decoction has been shown to ameliorate cognitive deficits, emerging as a promising intervention for Alzheimer's disease (AD) through its kidney-tonifying properties [14,15]. The combined use of SMS-LD has been employed to enhance cognitive functions, particularly learning and memory [16].

Erythropoietin (EPO) is recognized as a hematopoietic growth factor primarily produced by the kidneys [17], and it may serve as a critical component of the renal essence, known for its anti-inflammatory, antioxidant, anti-apoptotic, and angiogenic properties [18, 19]. Previous research has highlighted EPO's protective effects against neurodegenerative diseases, in addition to its well-documented role in hematopoiesis [20, 21]. The administration of EPO has been directly used to address hypoxic-ischemic encephalopathy [22] and has been implicated in the amelioration of cognitive dysfunction through treatments that tonify the kidney [23].

This study aimed to verify the therapeutic efficacy of SMS-LD on cognitive impairments induced by CIH and to propose a potential TCM treatment strategy for cognitive dysfunction in patients with OSA. This strategy emphasizes supplementing qi, nourishing yin, and strengthening the kidneys. We assessed the effects of SMS-LD on cognitive impairment in mice subjected to CIH, focusing on the neuroprotective role and the involvement of the EPO/EPOR/Janus kinase 2 (JAK2) signaling pathway. This research sought to lay the groundwork for clinical applications aimed at addressing cognitive impairments in patients with OSA.

Materials and Methods

Animals

Adult male C57BL/6N mice, aged 6−8 weeks and weighing 20−22 g, were sourced from the Beijing Vital River Laboratory Animal Technology Co., Ltd. (Beijing, China). Upon arrival, the animals were housed in a pathogen-free environment, maintained under a 12-hour light/dark cycle, and given ad libitum access to food and water. The experimental protocols were conducted in strict accordance with the National Institutes of Health Guide for the Care and Use of Laboratory Animals and received approval from the Animal Care and Use Committee of Hebei University of Chinese Medicine (Approval No. DWLL2020044).

The mice were randomly allocated into four groups: a normoxia control group (CON), a CIH, and two SMS-LD treatment groups receiving either a low dose (SMS-LD-L) or a high dose (SMS-LD-H). The CON group was subjected to normoxic conditions, while the CIH and SMS-LD groups were exposed to CIH conditions within a hypoxic chamber. The chamber's oxygen levels were cycled between 21% and 5% (5 min per cycle) for 8 h daily (9 : 00−17 : 00) for 35 days to mimic the CIH experienced during sleep by patients with OSA. This CIH model was established based on methodologies described in prior literature [24]. Specifically, the oxygen concentration was lowered to 5% by introducing 100% N_2 before being raised back to 21% by introducing 100% O_2, with each cycle lasting 5 min. The normoxia group was similarly placed in a chamber but was exposed to ambient air.

To simulate the therapeutic intervention, the mice in the SMS-LD groups received SMS-LD (at doses of 15.0 or 30.0 $g \cdot kg^{-1}$) *via* intragastric administration 30 min prior to daily CIH exposure. In parallel, mice in the CON and CIH groups were administered equal volumes of distilled water.

Cell culture

HT22 cells, acquired from Procell Life Science & Technology Co., Ltd. (Wuhan, China), were cultured in a cell incubator using a complete growth medium. These cells were categorized into five distinct groups: a CON, an IH group, an IH group treated with EPO, an IH group treated with a high dose of Shengmaisan and Liuwei Dihuang Decoction (SMS-LD-H) referred to as the SMS-LD group, and a group treated with AG490 (a JAK2 inhibitor) in combination with SMS-LD-H under IH conditions (AG490). HT22 cells in the CON group were maintained in a normoxic environment, whereas the cells in the other four groups underwent exposure to IH within a hypoxia chamber for 48 h, utilizing a protocol of 0.1% O_2 for 3 min followed by 21% O_2 for 7 min, at a rate of 6 cycles per hour. The EPO group received EPO at a final concentration of 10 $IU \cdot mL^{-1}$. The SMS-LD group was treated with 10% SMS-LD medicated serum. In the AG490 group, cells were treated with both 10% SMS-LD medicated serum and a final concentration of 50 $\mu mol \cdot L^{-1}$ AG490, the JAK2 inhibitor, to evaluate the combined effects on cellular response under IH conditions.

Antibodies and reagents

Antibodies against nuclear factor (erythroid-derived 2)-like 2 (Nrf2, 66504-1-Ig), phosphoinositide-3-kinase (PI3K, 20584-1-AP), phosphorylated protein kinase B (P-AKT,

66444-1-Ig), and AKT (10176-2-AP) were purchased from Proteintech (Rosemont, IL). Antibodies against EPO (GB11323), heme oxygenase 1 (HO-1, GB12104), Bcl-2-associated X protein (Bax, GB12690), PSD-95 (GB11277), brain-derived neurotrophic factor (BDNF, GB11559), and β-actin (GB12001) were purchased from Servicebio (Wuhan, China). The antibody against Bcl-2 (BA0412) was purchased from Boster (Wuhan, China). The antibody against Caspase-3 (#14220) was purchased from Cell Signaling Technology (Danvers, MA). Antibodies against dynamin-related protein 1 (Drp1, 221099) and optic atrophy 1 (Opa1, 382025) were purchased from Zenbioscience (Durham, NC). Antibodies against EPOR (DF7108), JAK2 (AF6022), P-JAK2 (AF3024), signal transducer and activator of transcription 5 (STAT5, DF3635), and P-STAT5 (AF3304) were purchased from Affinity (West Bedford, UK).

A reactive oxygen species (ROS) assay kit was obtained from Nanjing Jiancheng Bioengineering Institute (Nanjing, China). An active oxygen detection kit and mitochondrial membrane potential and apoptosis detection kit were purchased from Biyuntian Biotechnology Co., Ltd. (Shanghai, China). Exogenous EPO reagent (S20000026) was purchased from North China Pharmaceutical Jintan Biotechnology Co., Ltd.. JAK2 inhibitor AG490 (A4139) was purchased from APExBIO Co., Ltd.. All secondary antibodies and other regular reagents were obtained from Servicebio (Wuhan, China).

Preparation of SMS-LD

The composition of the Shengmaisan combined with Liuwei Dihuang Decoction (SMS-LD) includes the following herbs: 24 g of Rehmanniae Radix, 12 g of Dioscoreae Rhizoma, 12 g of Corni Fructus, 9 g of Moutan Cortex, 9 g of Alismatis Rhizoma, 9 g of Poria , 9 g of Ginseng, 9 g of Ophiopogonis Radix, and 6 g of Schisandrae Chinensis Fructus. For preparation, 99 g of these raw materials were initially soaked in 990 mL of distilled water for 30 min at room temperature, followed by boiling at 100 °C for 1 h. The resulting decoction was filtered and the residue was boiled again for another hour with 990 mL of distilled water. The two filtrates were combined and reduced to 100 mL under a water bath and then stored at 4 °C [8]. It is documented [25] that the yield from two rounds of decoction is approximately 75%. The conversion of doses between species, based on body surface area with a conversion coefficient (Km) of 12.3 for translating human doses to mice [26], results in an equivalent mouse dose of 99 g/60 kg × 75% × 12.3 = 15 g·kg^{-1}. Hence, in this study, the administered doses were defined as 15 g·kg^{-1}·day^{-1} for the low dose and 30 g·kg^{-1}·day^{-1} for the high dose.

Preparation of SMS-LD medicated serum

Twenty male C57/BL6N mice (6−8 weeks of age, body mass 20 ± 2 g) were purchased from Beijing Vital River Laboratory Animal Technology Corporation, Beijing, China. The mice were administered 30 g·kg^{-1}·day^{-1} of SMS-LD by intragastric administration for 7 d. At 1 h after the end of intragastric administration on day 7, blood was collected from the inner canthus of each mouse, and the SMS-LD medicated serum was obtained by centrifugation, inactivation, and sterilization.

Morris water maze

The Morris water maze, as detailed in our earlier study [27], consisted of a circular pool measuring 120 cm in diameter and 45 cm in height, filled with water maintained at a temperature of 21 ± 1 °C. During the testing phase, mice were required to use cues to locate a submerged escape platform from their starting position, with measurements taken of both the escape latency and swimming speed [28]. Following the removal of the platform, the mice's swimming trajectories were automatically documented using the Animal Video Analysis System (SMART 3.0, Panlab, Spain).

Intracerebroventricular injection

The mice were anesthetized and secured in motorized stereotaxic frames (Stoelting, IL, USA) for precise neurological interventions. AG490, a specific inhibitor of JAK2 phosphorylation, was prepared by dissolving it in dimethyl sulfoxide (DMSO) to achieve a final concentration of 5 mmol·L^{-1}. Each mouse received a stereotaxic injection of 5 mmol·L^{-1} AG490 (2 μL per mouse) directly into the lateral ventricle, adhering to the coordinates anteroposterior −0.34 mm, lateral −1.0 mm, and depth −2.2 mm [29]. Following a 30-minute waiting period to ensure AG490 uptake, the mice were subjected to CIH. To verify the accuracy of the injection sites at the conclusion of the study, 2% Chicago Sky Blue 6B dye (2 μL) was administered through the cannula into the same coordinates.

Golgi-Cox staining

The brains of anesthetized mice were promptly excised and then fixed in specimen bottles containing 20 mL of 4% paraformaldehyde following heart perfusion with 0.9% saline solution. Subsequent to fixation through maceration, the brains were placed in 50 mL amber glass bottles with 10 mL of Golgi-Cox solution and left to incubate for two weeks. After this period, the brains were immersed in a 30% sucrose solution for three days to ensure thorough cryoprotection. Coronal sections of the hippocampus were then prepared using a vibratome. These sections underwent a rinsing process with distilled water, followed by dehydration, and were finally encapsulated with glycerol gelatin. The density of dendritic spines within the hippocampal region was carefully examined and documented.

Transmission electron microscopy

The ultrastructural analysis of mitochondria was conducted using transmission electron microscopy. Following anesthesia, hippocampal tissues were swiftly excised and immediately submerged in a fixative solution specially formulated for electron microscopy. These tissues were then subjected to a dehydration process and subsequently embedded in epoxy resin for stabilization. Thin sections of the hippocampus were prepared using a vibratome, ensuring precise cuts for detailed examination. These sections were treated with double staining using uranyl acetate and lead nitrate to enhance con-

trast, facilitating the observation of mitochondrial structures. Finally, the stained sections were examined and imaged under an electron microscope, allowing for detailed observation of the mitochondrial ultrastructure.

Dihydroethidium (DHE) staining

Frozen tissue sections, prepared to a thickness of 5 μm, were stained using DHE following the guidelines provided by the staining kit. Subsequently, the nuclei within these sections were stained for 10 min using a DAPI staining solution. The final step involved the observation of the stained sections under a fluorescence microscope, allowing for the detailed visualization of the cellular and subcellular structures.

Immunohistochemistry

Seahorse paraffin sections were first placed in an oven set at 60 °C for 1 h, followed by a gradual dewaxing in xylene and a series of ethanol dilutions. The sections were then rinsed with phosphate-buffered saline (PBS) and treated with 3% hydrogen peroxide to quench endogenous peroxidase activity. After another PBS wash, the sections underwent antigen retrieval using a repair solution at a high temperature. Subsequently, the sections were blocked with 10% goat serum at room temperature for 60 min to prevent non-specific binding. Primary antibodies against EPO or EPO receptor (EPOR) were applied, and the sections were incubated overnight at 4 °C. Following this incubation, the sections were treated with HRP-conjugated (Horseradish Peroxidase) rabbit antibodies at 37 °C for 60 min. The immunohistochemistry analyses were completed with 3,3'-diaminobenzidine (DAB) staining to visualize the antigen-antibody complexes.

Cell vitality assay

Cell viability was assessed using the Cell Counting Kit-8 (CCK-8) method. HT22 cells were plated at a density of 1×10^4 cells per well in 96-well plates. After cell adhesion, the culture medium in each well was replaced with 100 μL of serum-free incubation solution, and the cells were subjected to either normoxic or IH conditions for 48 h. In the treatment groups, 1 μL of EPO (1000 IU·mL^{-1}) was added to achieve a final concentration of 10 IU·mL^{-1} in the EPO group, 10 μL of SMS-LD medicated serum (10%) was added to the SMS-LD group, and for the AG490 group, 10 μL of SMS-LD medicated serum (10%) and 1 μL of AG490 (5 mmol·L^{-1}) were added to reach a final concentration of 50 μmol·L^{-1}. After the 48-hour treatment period, 10 μL of CCK-8 solution was added to each well, and the plates were incubated for an additional hour in the incubator. The optical density of each well was then measured at 450 nm using a microplate reader to determine cell viability.

Measurement of ROS production

The ROS content was assessed using an active oxygen detection kit. HT22 cells were seeded onto cell slides within 24-well plates at a density of 4×10^4 cells/well. After cell adhesion, the culture medium in each well was replaced with 1 mL of serum-free incubation solution, and the cells were subjected to either normoxic or IH conditions for 48 h. To the EPO treatment group, 10 μL of EPO (1000 IU·mL^{-1}) was added to achieve a final concentration of 10 IU·mL^{-1}. The SMS-LD treatment group received 100 μL of SMS-LD medicated serum (10%), while the AG490 group was treated with both 100 μL SMS-LD medicated serum (10%) and 10 μL AG490 (5 mmol·L^{-1}) to reach a final concentration of 50 μmol·L^{-1}. Following treatment, 1 μL of the DCFH-DA probe was added to each well as directed by the ROS detection kit's protocol. The fluorescent staining of the cells was then observed under a fluorescence microscope, and images were captured from five random fields of view for each sample. The fluorescence intensity was quantitatively analyzed using ImageJ software.

Mitochondrial membrane potential and apoptosis staining

The mitochondrial membrane potential and apoptosis in HT22 cells were evaluated using a kit designed for this purpose, following the manufacturer's guidance. The HT22 cells were seeded onto cell slides and placed into 24-well plates, with each well accommodating 4×10^4 cells. To each well, 188 μL of incubation buffer, 5 μL of Annexin V-FITC conjugate, 2 μL of Mito-Tracker Red CMXRos staining solution, and 5 μL of Hoechst 33342 staining solution were added. After gently mixing, the preparations were incubated for 30 min at room temperature, shielded from light exposure. The staining results were then observed under a fluorescence microscope, selecting 5 random visual fields for analysis. The fluorescence intensity of these fields was quantified using ImageJ software.

Western blotting assay

As detailed in our prior study [30], the hippocampus or HT22 cells were processed with a mixture of protease inhibitors and a phosphorylated protease inhibitor, specifically phenylmethylsulfonyl fluoride (PMSF), before centrifugation. The resultant supernatant was collected, and the protein extracts were prepared for electrophoresis by heating in a metal bath at 100 °C. Following electrophoresis, the separated proteins were transferred onto polyvinylidene fluoride (PVDF) membranes. These membranes were then blocked using 5% skim milk at 37 °C for 2 h, creating a non-reactive barrier to prevent non-specific binding. After blocking, the membranes were incubated overnight at 4 °C with primary antibodies targeting EPO, EPOR, PSD-95, BDNF, Opa1, Drp1, Nrf2, HO-1, PI3K, AKT, phosphorylated AKT (P-AKT), JAK2, phosphorylated JAK2 (P-JAK2), STAT5, and phosphorylated STAT5 (P-STAT5). Subsequently, the blots were exposed to horseradish peroxidase (HRP)-conjugated secondary antibodies for 2 h at room temperature to ensure the detection of the primary antibody-protein complexes. The detection and visualization of these complexes were achieved using the enhanced chemiluminescence (ECL) method. The mean grey values of the target bands were quantitatively analyzed using ImageJ software.

Statistical analysis

All data collected were analyzed by SPSS version 23.0 software (SPSS Inc., Chicago, IL) and presented as the mean ± SEM. One-way ANOVA was performed, followed by Tukey post hoc tests.

Results

SMS-LD treatment improved animal performance in the Morris water maze in mice exposed to CIH

The effect of SMS-LD on cognitive impairment was assessed by the Morris water maze. During the hidden platform training with the Morris water maze, the escape latency and swimming speed were analyzed. As reflected in Fig. 1A, on days 3−5, the escape latency of mice in the CIH group was significantly longer compared with the CON group (P < 0.01), but SMS-LD-L and SMS-LD-H treatment significantly shortened the escape latency compared with the CIH group (P < 0.05 or P < 0.01). As shown in Fig. 1B, there was no significant difference in swimming speed, suggesting that CIH exposure and SMS-LD treatment did not affect the exercise capacity of the animals.

As shown in Fig. 1C−1D, the number of platform crossings decreased in the CIH group compared with the CON group (P < 0.001), but it was improved in the SMS-LD-L or SMS-LD-H groups compared with the CIH group (P < 0.05 or P < 0.01). As shown in Fig. 1E−1F, the distance traveled and the time spent in the target quadrant were significantly decreased in the CIH group compared with the CON group (P < 0.001), but they increased in the SMS-LD-L and SMS-LD-H group compared with the CIH group (P < 0.05 or P < 0.01). As shown in Fig. 1G−1H, there were no significant differences in escape latency and swimming speed among all four groups in the visible platform test. The results revealed that SMS-LD treatment significantly improved cognitive impairment in mice exposed to CIH.

SMS-LD treatment increased spine density and improved mitochondria damage in the hippocampus of mice exposed to CIH

Mitochondrial dysfunctions, which are closely linked to alterations in synaptic plasticity, are pivotal in the development of cognitive impairments. Therefore, this study aimed to assess the influence of SMS-LD on synaptic and mitochondrial morphological changes under CIH conditions, utilizing electron microscopy for detailed observation. Fig. 2A−2B illustrate a significant reduction in spine density within the CIH group when compared with the CON group (P < 0.05), indicating synaptic deterioration associated with CIH exposure. However, treatment with both low (SMS-LD-L) and high (SMS-LD-H) doses of SMS-LD resulted in a notable in-

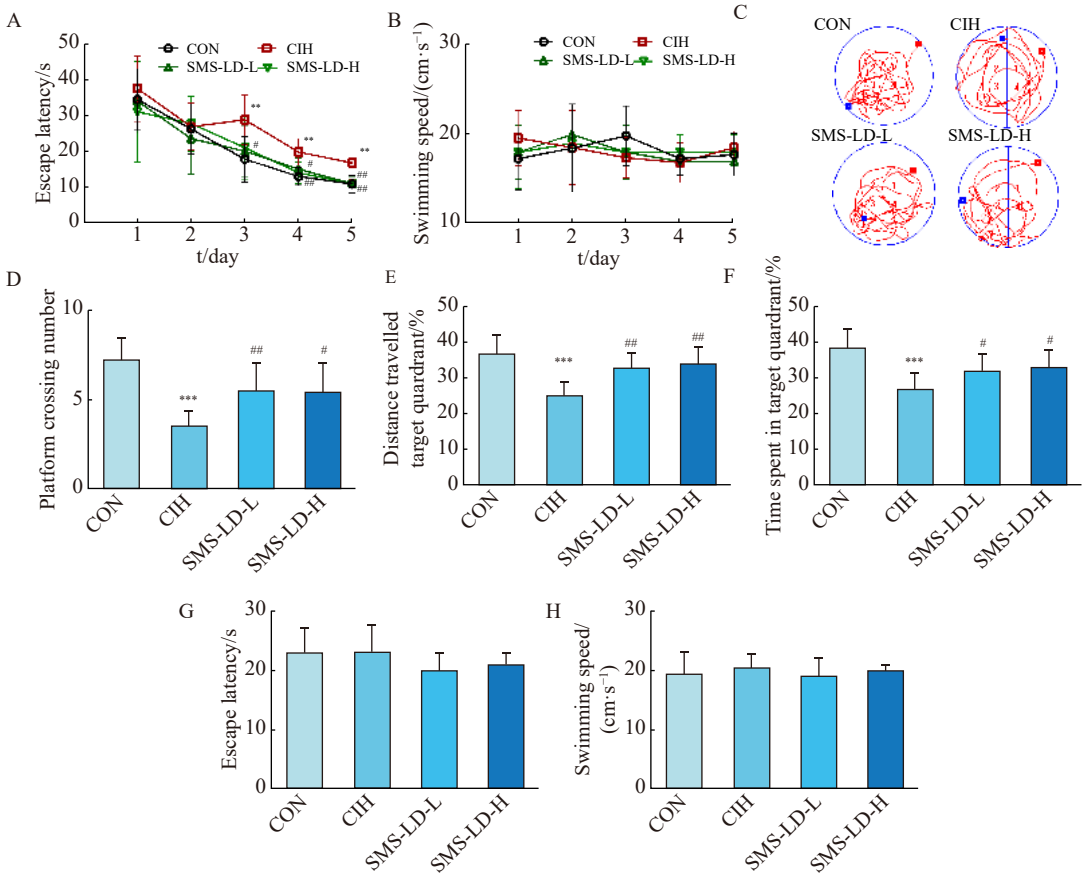

Fig. 1 Effect of SMS-LD treatment on cognitive impairment in mice exposed to CIH. (A) Escape latency in hidden platform training. (B) Swimming speed in hidden platform training. (C) Representative swimming tracks in the probe test. (D) Platform-crossing number in probe test. (E−F) Distance traveled in the target quadrant and time spent in the target quadrant in the probe test. (G−H) Escape latency and swimming speed in visible platform test. The results are presented as the mean ± SEM (n = 8 in eachgroup). $^{**}P$ < 0.01, $^{***}P$ < 0.001 *vs* the CON group, $^{\#}P$ < 0.05, $^{\#\#}P$ < 0.01 *vs* the CIH group.

crease in spine density compared with the CIH group ($P < 0.05$ or $P < 0.01$). Further analysis presented in Fig. 2C−2E revealed a considerable thinning of the PSD, along with damage to the mitochondrial structure, and reduced expressions of PSD-95 and BDNF in the CIH group compared with the CON group ($P < 0.05$). Conversely, treatments with SMS-LD-L and SMS-LD-H ameliorated these alterations, as evidenced by increases in PSD thickness, mitigation of mitochondrial damage, and enhanced expressions of PSD-95 and BDNF compared with the CIH group ($P < 0.05$ or $P < 0.01$).

As shown in Fig. 2F, Drp1 showed increased expression in the CIH group, while the expression of Opa1 was significantly reduced in the CIH group compared with the CON group ($P < 0.05$ or $P < 0.001$). Treatment with SMS-LD at both low (SMS-LD-L) and high (SMS-LD-H) doses resulted in a decrease in Drp1 expression and an increase in Opa1 expression compared with the CIH group ($P < 0.05$ or $P < 0.01$). These findings demonstrate that SMS-LD treatment effectively counters synaptic and mitochondrial damage induced by CIH in mice.

SMS-LD treatment attenuated oxidative stress in the hippocampus of mice exposed to CIH

Oxidative stress is mainly responsible for mitochondrial and synapse damage, especially under CIH conditions. As shown in Fig. 3A, the ROS production in the hippocampus of CIH mice was significantly increased, but it was significantly decreased by SMS-LD-L and SMS-LD-H treatment. As shown in Fig. 3B−3D, Nrf2 and HO-1 expressions in the hippocampus of CIH mice obviously declined compared with the CON group ($P < 0.05$ or $P < 0.01$), but this was obviously elevated by SMS-LD-L and SMS-LD-H treatment compared with the CIH group ($P < 0.05$ or $P < 0.001$). The results suggested that SMS-LD treatment significantly attenuates CIH-induced oxidative stress in the hippocampus.

SMS-LD treatment increased EPO and EPOR expressions in the hippocampus of mice exposed to CIH

EPO, serving as a crucial component of renal essence, has demonstrated potential in ameliorating cognitive dysfunction in mice. Aligning with the "kidney-marrow-brain" theory in TCM, the study explored the impact of SMS-LD on the expressions of EPO and its EPOR. As shown in Fig. 4A−4B, EPO expression in the hippocampus of the CIH group was lower compared with the CON group ($P < 0.01$), yet SMS-LD-L and SMS-LD-H treatments notably increased EPO expression relative to the CIH group ($P < 0.01$). Similarly, Fig. 4C−4D illustrate that EPOR expression was diminished in the CIH group when contrasted with the CON group ($P < 0.001$) but significantly elevated following both low and high doses of SMS-LD treatment ($P < 0.05$). These findings indicate that SMS-LD treatment effectively boosts EPO and EPOR expressions in the hippocampus of mice subjected to CIH, suggesting a therapeutic mechanism through which SMS-LD mitigates cognitive impairment associated with CIH.

Effect of SMS-LD treatment activated JAK2 signaling pathway in the hippocampus of mice exposed to CIH

To assess the activation impact of SMS-LD on the EPO/EPOR system, the downstream signaling pathway of EPOR was examined. Fig. 5A−5B illustrate that the phos-

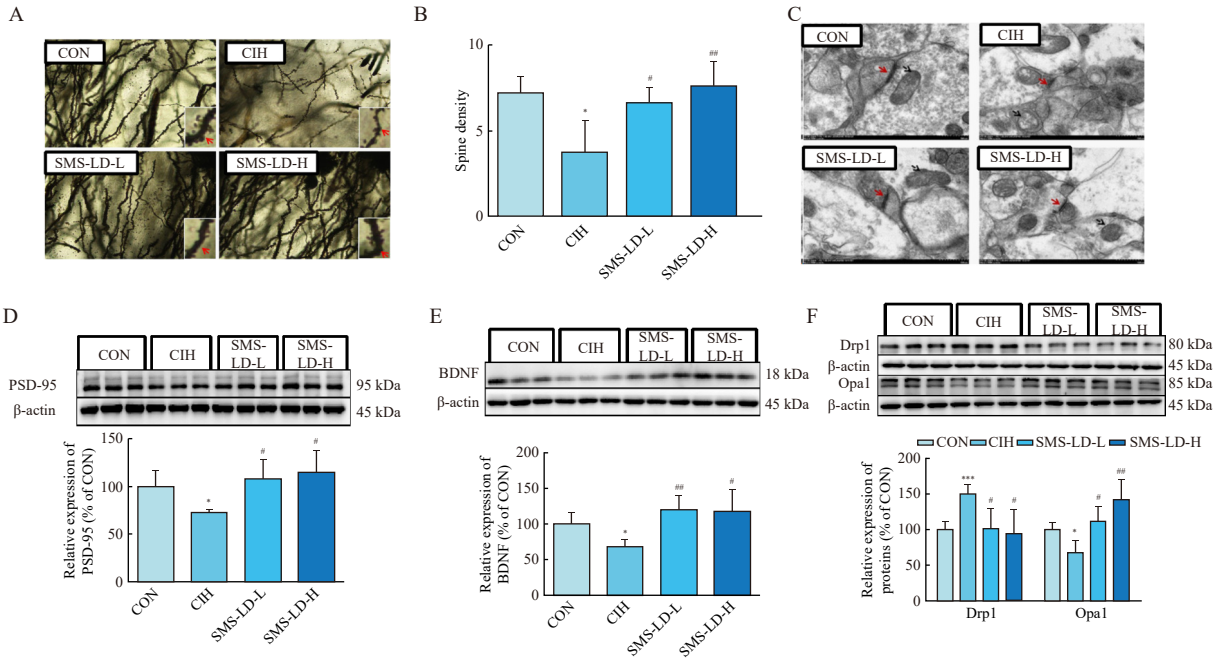

Fig. 2 Effects of SMS-LD treatment on synaptic morphology and mitochondria in the hippocampus of mice exposed to CIH. (A) Spine density in the hippocampus. (B) Calculated spine density in the hippocampus. (C) Images of mitochondria in the hippocampus. The red arrows indicate synapses, and the black arrows indicate mitochondria. (D−E) Expression of PSD-95 and BDNF proteins in the hippocampus. (F) Protein expression of Opa1 and Drp1 in the hippocampus. The results are presented as the mean ± SEM ($n = 6$ in each group), $^{*}P < 0.05$, $^{***}P < 0.001$ *vs* the CON group, $^{\#}P < 0.05$, $^{\#\#}P < 0.01$ *vs* the CIH group.

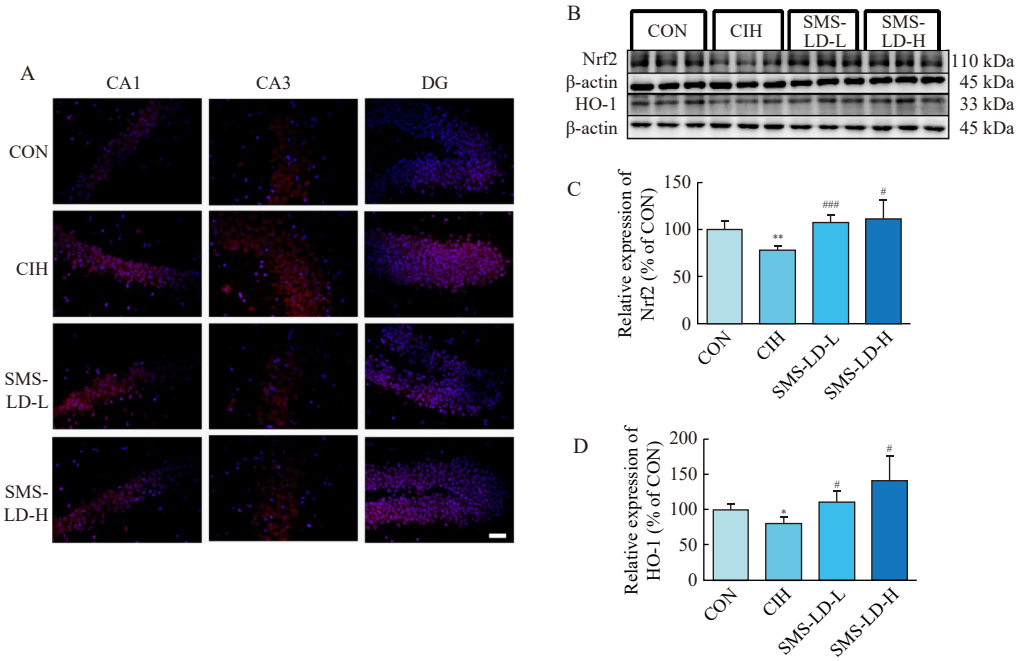

Fig. 3 Effects of SMS-LD on oxidative stress in the hippocampus of mice exposed to CIH. (A) DHE staining in the hippocampus (n = 3) (bar = 50 μm). (B) Western blotting bands of Nrf2 and HO-1 in the hippocampus. (C−D) Expressions of Nrf2 and HO-1 in the hippocampus. The results are presented as the mean ± SEM (n = 6), $^{*}P < 0.05$, $^{**}P < 0.01$ *vs* the CON group, $^{\#}P < 0.05$, $^{\#\#\#}P < 0.001$ *vs* the CIH group.

phorylation levels of JAK2 and STAT5 in the hippocampus were significantly lower in the CIH group compared with the CON group ($P < 0.01$ or $P < 0.001$). However, these levels were elevated in response to SMS-LD-L and SMS-LD-H treatments relative to the CIH group ($P < 0.05$ or $P < 0.001$).

Fig. 5C−5D show that both PI3K expression and the ratio of P-AKT to AKT in the hippocampus were notably reduced in the CIH group in comparison with the CON group ($P < 0.01$). Treatment with both low and high doses of SMS-LD resulted in increased PI3K expression and AKT phosphorylation compared with the CIH group ($P < 0.05$ or $P < 0.01$). These findings suggest that SMS-LD treatment effectively activates the JAK2 and STAT5 signaling pathways, as well as the PI3K-AKT pathway, in the hippocampus of mice subjected to CIH, contributing to the therapeutic effects observed in mitigating CIH-induced cognitive impairments.

SMS-LD treatment inhibited oxidative stress in HT22 cells exposed to IH by activating JAK2 signaling pathway

To elucidate the molecular mechanisms underlying the effects of SMS-LD, a study was conducted where HT22 cells exposed to IH for 48 h were treated with both SMS-LD medicated serum and a JAK2 inhibitor (AG490). The phosphorylation levels of JAK2 and STAT5 in HT22 cells were markedly reduced in the IH group compared with the CON group ($P < 0.01$). However, treatment with EPO and SMS-LD led to an increase in these phosphorylation levels compared with the IH group ($P < 0.05$ or $P < 0.01$). The introduction of AG490 prior to SMS-LD treatment effectively reversed the activation of JAK2 and STAT5 induced by SMS-LD ($P < 0.05$).

As shown in Fig. 6D−6F, regarding PI3K expression and AKT phosphorylation, significant reductions were observed in the IH group when compared with the CON group ($P < 0.05$ or $P < 0.01$). Treatments with EPO and SMS-LD were effective in increasing both PI3K expression and AKT phosphorylation relative to the IH group ($P < 0.05$). The use of AG490 prior to SMS-LD treatment reversed these increases ($P < 0.05$).

Furthermore, as illustrated in Fig. 6G−6H, ROS production was significantly higher in the IH group than in the CON group ($P < 0.001$) but was significantly reduced following treatment with EPO and SMS-LD ($P < 0.01$). AG490 pretreatment led to an increase in ROS levels compared with the SMS-LD-only group ($P < 0.05$).

Lastly, as shown in Fig. 6I−6K, the expressions of Nrf2 and HO-1 were significantly lower in the IH group compared with the CON group ($P < 0.01$) but showed significant increases following treatment with EPO and SMS-LD ($P < 0.05$ or $P < 0.01$). The introduction of AG490 before SMS-LD treatment reversed the increases in Nrf2 and HO-1 expressions ($P < 0.05$). These findings suggest that SMS-LD treatment mitigates oxidative stress in HT22 cells subjected to IH by activating the JAK2 signaling pathway.

SMS-LD treatment increased cell activity and inhibited cell apoptosis and mitochondrial damage in HT22 cells exposed to IH by activating JAK2 signaling pathway

Fig. 7A−7C demonstrates that the mitochondrial membrane potential was significantly lower and apoptosis markedly higher in the IH group compared with those in the CON group ($P < 0.05$). Treatment with EPO and SMS-LD

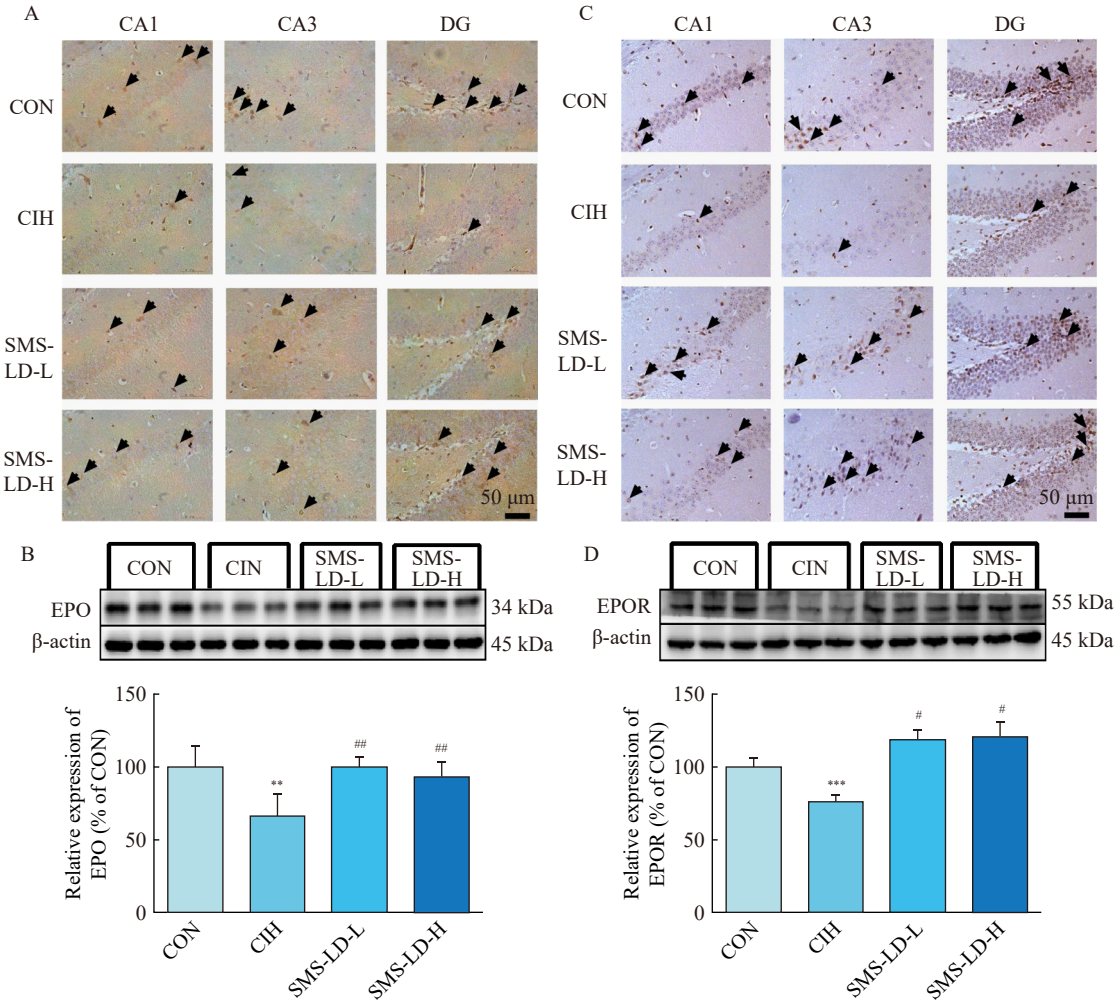

Fig. 4 Effects of SMS-LD treatment on EPO and EPOR expressions in the hippocampus of mice exposed to CIH. (A) Immunohistochemical staining of EPO in the hippocampus (n = 3). Black arrows mean positive expressions. (B) Expression of EPO in the hippocampus according to Western blotting. (C) Immunohistochemical staining of EPOR in the hippocampus (n = 3). Black arrows mean positive expressions. (D) Expression of EPOR in the hippocampus according to Western blotting. The results are presented as the mean ± SEM (n = 6), $^{*}P < 0.05$, $^{***}P < 0.001$ *vs* the CON group, $^{\#}P < 0.05$, $^{\#\#}P < 0.01$ *vs* the CIH group.

notably improved mitochondrial membrane potential and reduced apoptosis levels in comparison to the IH group ($P < 0.05$ or $P < 0.01$). However, pre-treatment with AG490 before SMS-LD application resulted in a decrease in mitochondrial membrane potential and an increase in apoptosis compared with the SMS-LD-treated group ($P < 0.05$).

As depicted in Fig. 7D, the optical density (OD) value, indicative of cell activity, was significantly lower in the IH group than in the CON group ($P < 0.001$). Treatment with EPO and SMS-LD significantly enhanced cell activity relative to the IH group ($P < 0.01$). AG490 pre-treatment led to a reduction in cell activity compared with the group treated with SMS-LD alone ($P < 0.001$). Fig. 7E−7G reveal changes in mitochondrial dynamics proteins, with Opa1 expression being significantly lower and Drp1 expression significantly higher in the IH group compared with the CON group ($P < 0.05$ or $P < 0.01$). EPO and SMS-LD treatments significantly increased Opa1 and decreased Drp1 expressions compared with the IH group ($P < 0.05$ or $P < 0.01$). AG490 pre-treatment reversed these effects, leading to decreased Opa1 and increased Drp1 expressions compared with the SMS-LD-treated group ($P < 0.05$).

Lastly, as illustrated in Fig. 7H−7J, Bcl-2/Bax was significantly decreased, and cleaved caspase-3/caspase-3 was significantly increased in the IH group compared with the CON group ($P < 0.05$ or $P < 0.01$). Bcl-2/Bax was significantly increased and cleaved caspase-3/caspase-3 was significantly decreased after EPO and SMS-LD treatment compared with the IH group ($P < 0.05$ or $P < 0.01$). Pre-treatment with AG490 decreased Bcl-2/Bax and increased cleaved caspase-3/caspase-3 compared with the SMS-LD group ($P < 0.05$). The results showed that SMS-LD treatment increased cell activity while it inhibited cell apoptosis and mitochondrial damage in HT22 cells exposed to IH by activating the JAK2 signaling pathway.

AG490 reversed the ameliorative effect of SMS-LD treatment on the Morris water maze in mice exposed to CIH

The Morris water maze was used to evaluate the impact

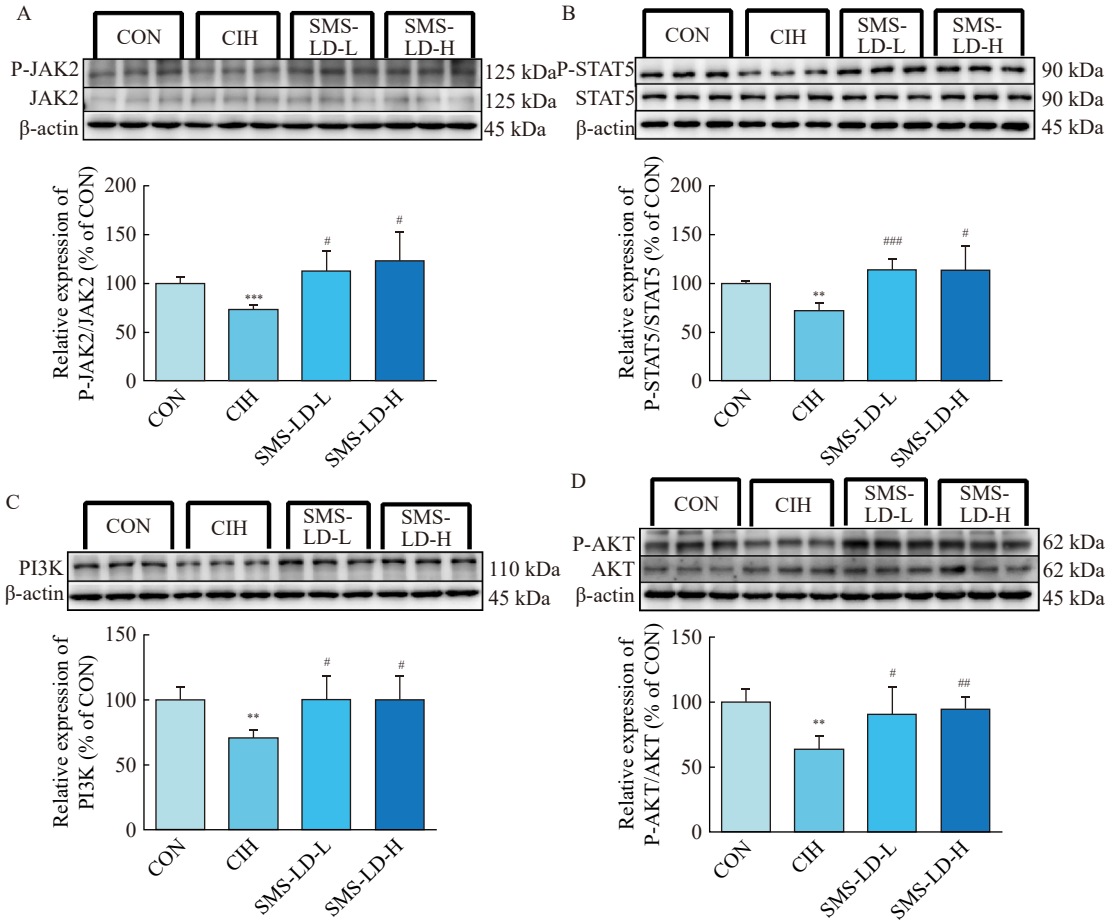

Fig. 5 Effects of SMS-LD treatment on JAK2-related signaling pathway in the hippocampus of mice exposed to CIH. (A) Expression of P-JAK2/JAK2 in the hippocampus. (B) Expression of P-STAT5/STAT5 in the hippocampus. (C) Expression of PI3K in the hippocampus. (D) Expression of P-AKT/AKT in the hippocampus. The results are presented as the mean ± SEM (n = 6), $^{**}P < 0.01$, $^{***}P < 0.001$ *vs* the CON group, $^{\#}P < 0.05$, $^{\#\#}P < 0.01$, $^{\#\#\#}P < 0.001$ *vs* the CIH group.

of AG490 on cognitive impairment. The analysis focused on escape latency and swimming speed. Fig. 8A indicates that, during days 3−5, the CIH group exhibited significantly longer escape latencies compared with the CON group ($P < 0.01$), a discrepancy significantly mitigated by SMS-LD-H treatment ($P < 0.01$ or $P < 0.001$). However, the administration of AG490 *via* intracerebroventricular injection counteracted the reduction in escape latency achieved by SMS-LD-H treatment ($P < 0.05$ or $P < 0.01$). Fig. 8B shows no significant difference in swimming speed, implying that neither CIH exposure nor intracerebroventricular injection impacted the animals' physical capacity.

Fig. 8C−8D demonstrate a decrease in the number of platform crossings for the CIH group relative to the CON group ($P < 0.001$), an outcome that was significantly improved by SMS-LD-H treatment ($P < 0.001$). However, AG490 treatment reversed this improvement ($P < 0.01$). Fig. 8E−8F reveal that both the distance traveled and time spent in the target quadrant were notably less in the CIH group compared with the CON group ($P < 0.001$), yet these metrics were enhanced in the SMS-LD-H group relative to the CIH group ($P < 0.01$), with AG490 reversing these enhancements ($P < 0.05$ or $P < 0.001$). Fig. 8G−8H indicate no significant differences in escape latency and swimming speed across all groups in the visible platform test. These results suggest that AG490 reverses the positive effects of SMS-LD treatment on cognitive impairment in mice subjected to CIH.

Discussion

In recent years, OSA has emerged as a prevalent condition with far-reaching health and safety implications [31]. Currently, there is no definitive medical treatment for the cognitive dysfunctions induced by OSA[32]. Within TCM, cognitive impairment, closely linked to dementia, is traditionally managed through nourishing yin and tonifying the kidneys. The combination of SMS-LD is recognized in TCM for its ability to supplement qi, nourish yin, and strengthen the kidneys, and is frequently applied in treating DQYS [33, 34].

CIH serves as a reliable model for mimicking the hypoxia/reoxygenation episodes experienced by OSA patients and is extensively utilized in research [35, 36]. Studies have reported that mice subjected to CIH exhibit symptoms characteristic of DQYS, including emaciation, weakness, anorexia, thirst, and irritability [8, 24]. This study assessed the therapeutic impact of SMS-LD on CIH-induced cognitive impairments us-

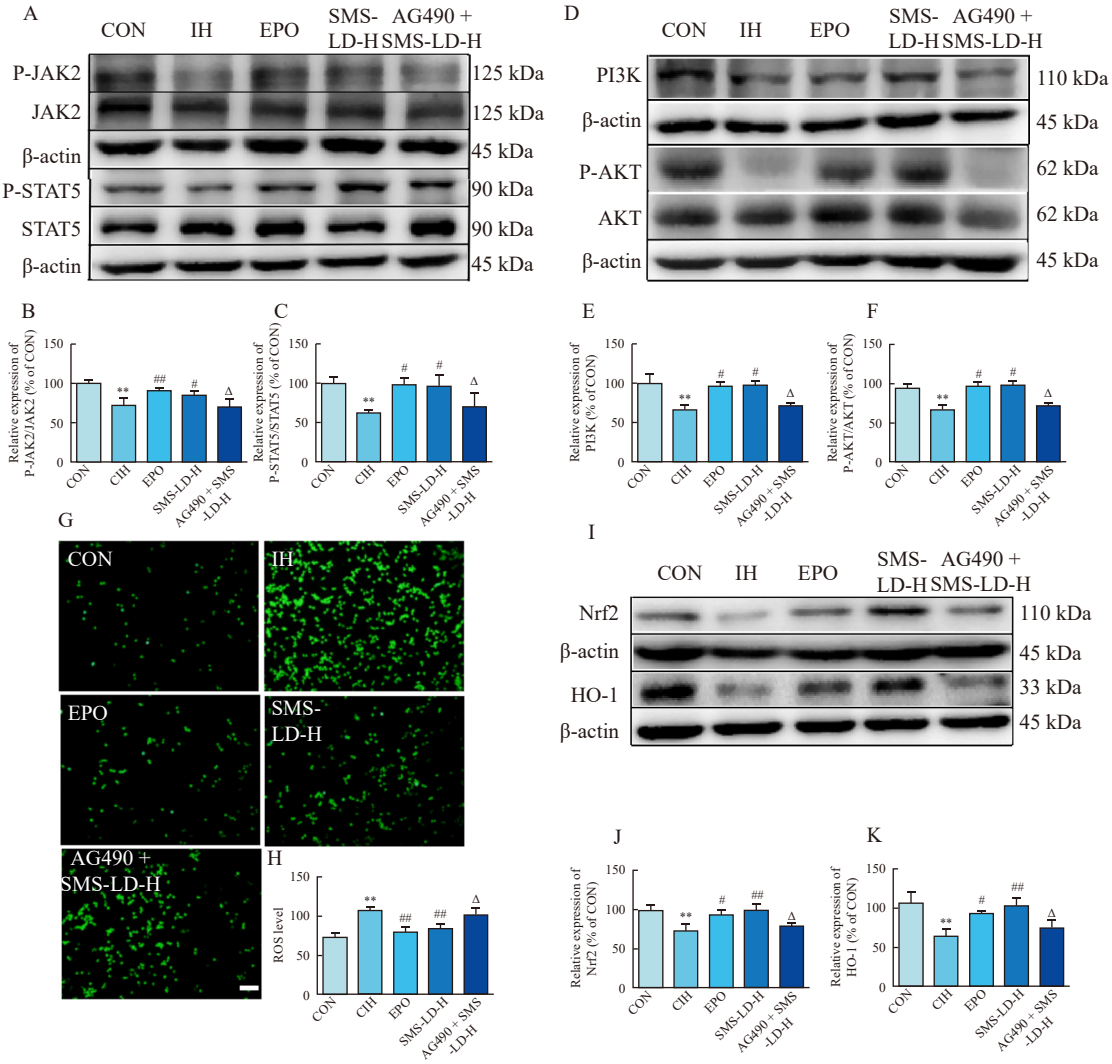

Fig. 6 Effects of SMS-LD treatment on JAK2-related signaling pathway and oxidative stress in HT22 cells exposed to IH. (A) Western blotting bands of JAK2 and STAT5 in HT22 cells. (B) Expression of P-JAK2/JAK2 in HT22 cells. (C) Expression of P-STAT5/STAT5 in HT22 cells. (D) Western blotting bands of PI3K and AKT in HT22 cells. (E) Expression of PI3K in HT22 cells. (F) Expression of P-AKT/AKT in HT22 cells. (G) ROS production in HT22 cells exposed to IH (bar = 50 μm). (H) Oxidative stress level in HT22 cells exposed to IH. (I) Western blotting bands of Nrf2 and HO-1 in HT22 cells. (J) Expression of Nrf2 in HT22 cells. (K) Expression of HO-1 in HT22 cells. The results are presented as the mean ± SEM (n = 3), $^{*}P < 0.05$, $^{**}P < 0.01$, $^{***}P < 0.001$ *vs* the CON group, $^{\#}P < 0.05$, $^{\#\#}P < 0.01$ *vs* the IH group, $^{\triangle}P < 0.05$, $^{\triangle\triangle}P < 0.01$ *vs* the SMS-LD group.

ing the Morris water maze, revealing significant enhancements in maze performance, thus proposing SMS-LD as a potential TCM-based strategy for addressing cognitive dysfunctions in OSA patients.

In the CIH group, the distance traveled, time spent in the target quadrant, and the number of platform crossings were significantly decreased, and the escape latency was longer, which is consistent with previous studies. SMS-LD treatment improved CIH-induced cognitive impairment by improving the mice's maze performance. Thus, SMS-LD could provide a potential TCM treatment strategy targeting cognitive dysfunction in patients with OSA.

Mitochondrial health is crucial for brain functions, including cognition, through its influence on synaptic transmission [37]. The association between mitochondrial damage and cognitive impairment is attributed to disrupted synaptic plasticity [38]. BDNF and PSD-95 are critical for synaptic transmission and neuron/synaptic plasticity and essential for learning and memory [39, 40], with EPO known to upregulate neurotrophic factors like BDNF and PSD-95 [41, 42]. BDNF plays a pivotal role in synaptic plasticity, neuron survival, proliferation, and even in neuronal death [43] and is recognized for its cognitive enhancement capabilities [44, 45].

PSD-95 is crucial for synaptic maturation, stability, and memory formation [46, 47], with its overexpression linked to improved synaptic plasticity [48]. Our findings demonstrated reductions in spine density, mitochondrial health, and expressions of BDNF and PSD-95 in the CIH group, alongside mitochondrial structural damage. SMS-LD treatment ameliorated these issues, enhancing spine density, BDNF, and PSD-

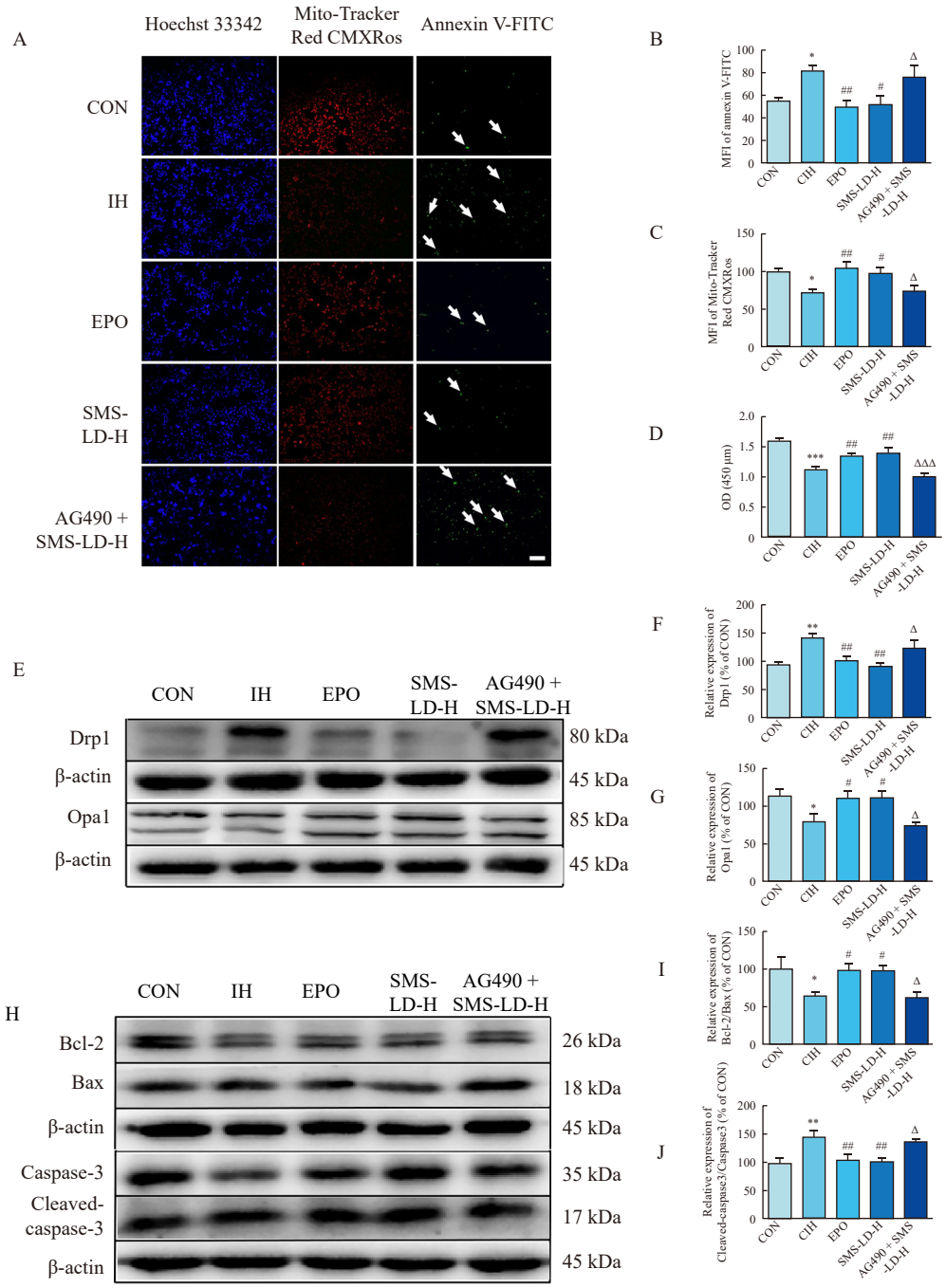

Fig. 7 Effects of SMS-LD on cell activity, cell apoptosis, and mitochondrial damage in HT22 cells exposed to IH. (A−C) Mitochondrial membrane potential and cell apoptosis level in HT22 cells exposed to IH. Arrows indicate positive cells (bar = 50 μm). (D) OD value in HT22 cells exposed to IH. (E) Western blotting bands of Drp1 and Opa1 in HT22 cells. (F) Expression of Drp1 in HT22 cells. (G) Expression of Opa1 in HT22 cells. (H) Western blotting bands of Bcl-2/Bax and cleaved caspase-3/caspase-3 in HT22 cells. (I) Expression of Bcl-2/Bax in HT22 cells. (J) Expression of cleaved caspase-3/caspase-3 in HT22 cells. The results are presented as the mean ± SEM (n = 3), $^{*}P < 0.05$, $^{**}P < 0.01$, $^{***}P < 0.001$ *vs* the CON group, $^{\#}P < 0.05$, $^{\#\#}P < 0.01$ *vs* the IH group, $^{\triangle}P < 0.05$, $^{\triangle\triangle\triangle}P < 0.001$ *vs* the SMS-LD group.

95 expressions in the hippocampus, pointing to its neuroprotective effects.

The hippocampus, vital for memory, shows particular vulnerability to both prolonged and IH associated with sleep conditions like OSA[49, 50]. The cognitive impairments linked to OSA are primarily driven by oxidative stress and apoptosis within the hippocampus [51]. Repetitive hypoxia/reoxygenation cycles are known to foster oxidative stress and apoptosis [52], with hippocampal oxidative stress implicated in memory deficits in rodent models [53].

Nrf2 emerges as a crucial regulator of cellular antioxidant defenses [54], with its ability to regulate antioxidant pro-

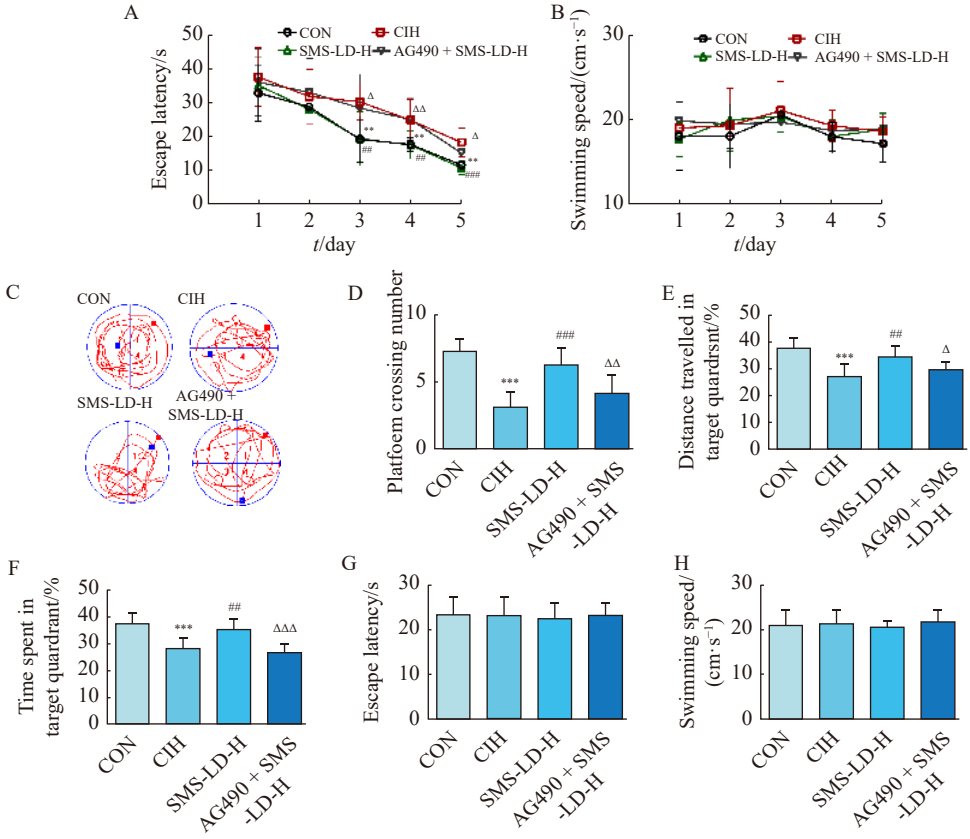

Fig. 8 AG490 reversed the ameliorative effect of SMS-LD treatment on the Morris water maze in mice exposed to CIH. (A) Escape latency in hidden platform training. (B) Swimming speed in hidden platform training. (C) Representative swimming tracks in the probe test. (D) Platform-crossing number in the probe test. (E−F) Distance traveled in the target quadrant and time spent in the target quadrant in the probe test. (G−H) Escape latency and swimming speed in the visible platform test. The results are presented as the mean ± SEM (n = 8 in each group). $^{**}P < 0.01$, $^{***}P < 0.001$ *vs* the CON group, $^{\#\#}P < 0.01$, $^{\#\#\#}P < 0.001$ *vs* the CIH group. $^{\triangle}P < 0.05$, $^{\triangle\triangle}P < 0.01$, $^{\triangle\triangle\triangle}P < 0.001$ *vs* the SMS-LD-H group.

tein expressions, reduce ROS production, and mitigate oxidative damage being extensively documented [55]. Overexpression of Nrf2 has been shown to improve spatial learning and memory in AD mouse models, underscoring its potential therapeutic relevance [56].

The antioxidant enzyme HO-1 plays a crucial protective role in mitigating oxidative stress and enhancing cognitive function [57, 58], with activation by Nrf2 potentially inhibiting the oxidative reactions induced by CIH in neurodegeneration [59, 60]. Previous research has demonstrated that CIH-induced oxidative stress leads to reduced expressions within the Nrf2/HO-1 pathway. In our investigation, we observed a significant increase in ROS production and a marked decrease in Nrf2 and HO-1 expressions in the hippocampus of CIH-exposed mice. These adverse effects were notably ameliorated by treatments with both low and high doses of SMS-LD, suggesting that the therapeutic effects of SMS-LD may be mediated through the Nrf2-HO-1 pathway, thereby reducing oxidative stress and improving cognitive impairments.

In TCM, cognitive impairment, commonly associated with dementia, is thought to arise from a deficiency in cerebral nutrition. There is a recognized connection between the kidneys and brain, with renal function playing a key role in maintaining overall body and neuronal homeostasis [61]. EPO, predominantly produced in the kidneys and found in both the kidneys and the brain [62], has been shown to confer protective effects against various nervous system diseases experimentally and improve cognitive dysfunction in mice [63]. The EPOR, present in the brain, plays a neuroprotective role in ischemic and neurodegenerative diseases [64].

Research has highlighted the cognitive protective effects of Liuwei Dihuang decoction and its principal component, Radix Rehmanniae, through the replenishment of kidney essence [65-68]. Catalpol, a major active compound in Radix Rehmanniae, has been found to enhance the expressions of EPO and EPOR, contributing to cognitive improvement [69-71]. Our study observed that expressions of EPO and EPOR in the hippocampus of CIH mice were significantly reduced, an effect which was reversed by SMS-LD treatments, hinting at the potential of SMS-LD to ameliorate cognitive impairments through the EPO-EPOR pathway, albeit with the precise mechanism remaining to be elucidated.

EPO also exerts significant neuroprotective actions through the activation of the JAK2 pathway and mitigates ox-

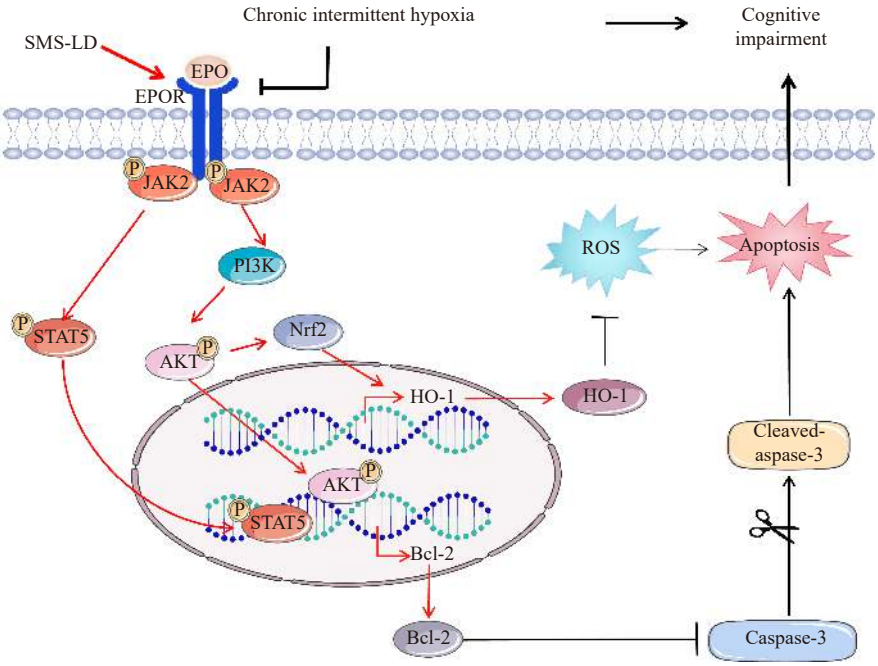

Fig. 9 Neuroprotective mechanism of SMS-LD treatment on CIH-induced cognitive impairment through activating the EPO/EPOR/JAK2 signaling pathway.

idative stress by stimulating the JAK2-STAT5 and PI3K-AKT pathways, crucial in the context of stroke [72]. The activation of JAK2 leads to the activation of several other kinases, including PI3K/AKT and the STAT family of transcription factors [73, 74], which have been shown to counter oxidative stress [75]. The PI3K-AKT pathway, an essential factor in antioxidant defense, activates expressions of Nrf2 and HO-1, further reducing oxidative stress [76].

PI3K-AKT is an important antioxidant stress factor [77], activating the expression of Nrf2 and HO-1, which are key players in reducing oxidative stress [78, 79]. The pathways mediated by EPO, specifically JAK/STAT5 and PI3K/AKT, significantly influence neural health by regulating the Nrf2/HO-1 pathway, thereby mitigating oxidative stress [80, 81]. The PI3K-AKT pathway plays a crucial role as an antioxidant factor, activating the expression of Nrf2 and HO-1, which are key players in reducing oxidative stress. The pathways mediated by EPO, specifically JAK/STAT5 and PI3K/AKT, significantly influence neural health by regulating the Nrf2/HO-1 pathway, thereby mitigating oxidative stress. In our study, we observed that the expressions of PI3K and the ratios of phosphorylated to total AKT (P-AKT/AKT), JAK2 (P-JAK2/JAK2), and STAT5 (P-STAT5/STAT5) were notably decreased in the hippocampus of mice exposed to CIH. These alterations were significantly ameliorated by treatments with both low (SMS-LD-L) and high (SMS-LD-H) doses of Shengmaisan combined with Liuwei Dihuang decoction (SMS-LD), suggesting the potential of SMS-LD to counteract CIH-induced oxidative and neurodegenerative changes. By enhancing the EPO-mediated JAK/STAT5 and PI3K/AKT pathways, SMS-LD may effectively alleviate cognitive impairment, aligning with the "kidney-marrow-brain" theory in TCM. This approach underscores the significance of nourishing kidney essence for cognitive health and positions SMS-LD as a promising therapeutic strategy for cognitive impairment in patients with OSA.

Conclusion

This study demonstrated that treatment with SMS-LD significantly mitigated cognitive impairment in mice subjected to CIH. The primary mechanism underlying this effect appears to be the activation of the EPO/EPOR/JAK2 signaling pathway (Fig. 9). Additionally, our findings propose a potential TCM treatment approach aimed at addressing cognitive dysfunction in patients with OSA, highlighting the integration of traditional therapeutic wisdom with modern clinical needs.

Availability of data and materials

The data presented in the study may be made available from the corresponding author upon reasonable request.

References

[1] Shen YC, Kung SC, Chang ET, *et al*. The impact of obesity in cognitive and memory dysfunction in obstructive sleep apnea syndrome [J]. *Int J Obes (Lond)*, 2019, **43**(2): 355-361.
[2] Wang B, Li W, Jin H, *et al*. Curcumin attenuates chronic intermittent hypoxia-induced brain injuries by inhibiting AQP4 and p38 MAPK pathway [J]. *Respir Physiol Neurobiol*, 2018, **255**: 50-57.
[3] Vanek J, Prasko J, Genzor S, *et al*. Obstructive sleep apnea, depression and cognitive impairment [J]. *Sleep Med*, 2020, **72**: 50-58.
[4] Liu T, Ouyang R. Effect of continuous positive air pressure on cognitive impairment associated with obstructive sleep apnea [J]. *J Central South Univ*, 2021, **46**(8): 865-871.
[5] Seo YJ, Ju HM, Lee SH, *et al*. Damage of inner ear sensory

hair cells via mitochondrial loss in a murine model of sleep apnea with chronic intermittent hypoxia [J]. *Sleep*, 2017, **40**(9): zsx106.
[6] Afsar B, Sag AA, Yalcin CE, *et al*. Brain-kidney cross-talk: definition and emerging evidence [J]. *Eur J Intern Med*, 2016, **36**: 7-12.
[7] Gao SD, Deng YY, Wang CY, *et al*. The correlation and clinical significance of Kidney-Cone-Myeloid-Brain in China [J]. *J Practical Tradit Chin Internal Medi*, 2022, **36**(06): 44-47.
[8] Zhao Y, Yang S, Guo Q, *et al*. Shashen-Maidong Decoction improved chronic intermittent hypoxia-induced cognitive impairment through regulating glutamatergic signaling pathway [J]. *J Ethnopharmacol*, 2021, **274**: 114040.
[9] Tao F, Lu P, Xu C, *et al*. Metabolomics analysis for defining serum biochemical markers in colorectal cancer patients with Qi deficiency syndrome or Yin deficiency syndrome [J]. *Evid Based Complement Alternat Med*, 2017, **2017**: 7382752.
[10] Chen J, Wang S, Shen J, *et al*. Analysis of gut microbiota composition in lung adenocarcinoma patients with TCM Qi-Yin deficiency [J]. *Am J Chin Med*, 2021, **49**(7): 1667-1682.
[11] Mo WL, Chai CZ, Kou JP, *et al*. Sheng-Mai-San attenuates contractile dysfunction and structural damage induced by chronic intermittent hypoxia in mice [J]. *Chin J Nat Med*, 2015, **13**(10): 743-50.
[12] He Q, Zhang QJ. Clinical efficacy of Shengmaisan in the treatment of Qi Yin deficiency syndrome of novel coronavirus pneumonia in convalescent stage [J]. *Acta Chin Med Pharm*, 2021, **49**(03): 84-86.
[13] Lu YL. To explore the curative effect of Shengmaisan Decoction in the treatment of type 2 diabetes with T2DM Qi Yin deficiency syndrome combined with coronary heart disease and angina pectoris [J]. *Contemp Med*, 2021, **27**(33): 131-132.
[14] Liu B, Chen B, Yi J, *et al*. Liuwei Dihuang Decoction alleviates cognitive dysfunction in mice with D-galactose-induced aging by regulating lipid metabolism and oxidative stress *via* the microbiota-gut-brain axis [J]. *Front Neurosci*, 2022, **16**: 949298.
[15] Cheng X, Huang Y, Zhang Y, *et al*. LW-AFC, a new formula from the traditional Chinese medicine Liuwei Dihuang decoction, as a promising therapy for Alzheimer's disease: pharmacological effects and mechanisms [J]. *Adv Pharmacol*, 2020, **87**: 159-177.
[16] Liu NB, Liu XQ, Liu SC, *et al*. Study on the effect of Shengmai Yin and Liuwei Dihuang Wan on improving learning and memory disorders induced by chronic stress [J]. *Liaoning J Tradit Chin Medi*, 2002, (01): 1-3.
[17] Zhang XB, Zeng YM, Zeng HQ, *et al*. Erythropoietin levels in patients with sleep apnea: a meta-analysis [J]. *Eur Arch Otorhinolaryngol*, 2017, **274**(6): 2505-2512.
[18] Merelli A, Czornyj L, Lazarowski A. Erythropoietin as a new therapeutic opportunity in brain inflammation and neurodegenerative diseases [J]. *Int J Neurosci*, 2015, **125**(11): 793-797.
[19] Siren AL, Fratelli M, Brines M, *et al*. Erythropoietin prevents neuronal apoptosis after cerebral ischemia and metabolic stress [J]. *Proc Natl Acad Sci U S A*, 2001, **98**(7): 4044-9.
[20] Sun J, Martin JM, Vanderpoel V, *et al*. The promises and challenges of erythropoietin for treatment of Alzheimer's disease [J]. *Neuromol Med*, 2019, **21**(1): 12-24.
[21] Wilms H, Schwabedissen B, Sievers J, *et al*. Erythropoietin does not attenuate cytokine production and inflammation in microglia-implications for the neuroprotective effect of erythropoietin in neurological diseases [J]. *J Neuroimmunol*, 2009, **212**(1-2): 106-11.
[22] Oorschot DE, Sizemore RJ, Amer AR. Treatment of neonatal hypoxic-ischemic encephalopathy with erythropoietin alone, and erythropoietin combined with hypothermia: history, current status, and future research [J]. *Int J Mol Sci*, 2020, **21**(4): 1487.
[23] Tang Q, Ke H, Wu C, *et al*. Aqueous extract from You-Gui-Yin ameliorates cognitive impairment of chronic renal failure mice through targeting hippocampal CaMKIIalpha/CREB/BDNF and EPO/EPOR pathways [J]. *J Ethnopharmacol*, 2019, **239**: 111925.
[24] Zheng Y, Yang S, Si J, *et al*. Shashen-Maidong Decoction inhibited cancer growth under intermittent hypoxia conditions by suppressing oxidative stress and inflammation [J]. *J Ethnopharmacol*, 2022, **299**: 115654.
[25] Liu HY, Wu ST. Dosage conversion of classical prescription [J]. *Chin J Tradit Chin Med Pharm*, 2014, **29**(04): 1007-1009.
[26] Nair A, Morsy MA, Jacob S. Dose translation between laboratory animals and human in preclinical and clinical phases of drug development [J]. *Drug Dev Res*, 2018, **79**(8): 373-382.
[27] Yang S, Wen D, Dong M, *et al*. Effects of cholecystokinin-8 on morphine-induced spatial reference memory impairment in mice [J]. *Behav Brain Res*, 2013, **256**: 346-53.
[28] Gibson BM, Mair R. A pathway for spatial memory encoding [J]. *Learn Behav*, 2016, **44**(2): 97-98.
[29] Payolla TB, Lemes SF, de Fante T, *et al*. High-fat diet during pregnancy and lactation impairs the cholinergic anti-inflammatory pathway in the liver and white adipose tissue of mouse offspring [J]. *Mol Cell Endocrinol*, 2016, **422**: 192-202.
[30] An JR, Zhao YS, Luo LF, *et al*. Huperzine A, reduces brain iron overload and alleviates cognitive deficit in mice exposed to chronic intermittent hypoxia [J]. *Life Sci*, 2020, **250**: 117573.
[31] Garbarino S, Scoditti E, Lanteri P, *et al*. Obstructive sleep apnea with or without excessive daytime sleepiness: clinical and experimental data-driven phenotyping [J]. *Front Neurol*, 2018, **9**: 505.
[32] Andrade AG, Bubu OM, Varga AW, *et al*. The relationship between obstructive sleep apnea and Alzheimer's Disease [J]. *J Alzheimers Dis*, 2018, **64**(s1): S255-S270.
[33] Zhang H, Zhou Q, Wang S. Effect of Shengmai Powder and Liuwei Dihuang Pill in the treatment of Type 2 diabetes with deficiency of Qi and Yin [J]. *Health Everyone*, 2020, (05): 284.
[34] Mei C, Zhang L, Zhang SS. Clinical Study on Shengmai Powder and Liuwei Dihuang Tang for Type 2 Diabetes of Qi-yin Deficiency Type [J]. *N Chin Med*, 2019, **51**(07): 93-96.
[35] Gong LJ, Wang XY, Gu WY, *et al*. Pinocembrin ameliorates intermittent hypoxia-induced neuroinflammation through BNIP3-dependent mitophagy in a murine model of sleep apnea [J]. *J Neuroinflammation*, 2020, **17**(1): 337.
[36] Dumitrascu R, Heitmann J, Seeger W, *et al*. Obstructive sleep apnea, oxidative stress and cardiovascular disease: lessons from animal studies [J]. *Oxid Med Cell Longev*, 2013, **2013**: 234631.
[37] Picard M, McEwen BS. Mitochondria impact brain function and cognition [J]. *Proc Natl Acad Sci U S A*, 2014, **111**(1): 7-8.
[38] Jang Y, Lee JH, Lee MJ, *et al*. Schisandra extract and ascorbic acid synergistically enhance cognition in mice through modulation of mitochondrial respiration [J]. *Nutrients*, 2020, **12**(4): 897.
[39] Nikolaienko O, Patil S, Eriksen MS, *et al*. Arc protein: a flexible hub for synaptic plasticity and cognition [J]. *Semin Cell Dev Biol*, 2018, **77**: 33-42.
[40] Todorova V, Blokland A. Mitochondria and synaptic plasticity in the mature and aging nervous system [J]. *Curr Neuropharmacol*, 2017, **15**(1): 166-173.
[41] Viviani B, Bartesaghi S, Corsini E, *et al*. Erythropoietin protects primary hippocampal neurons increasing the expression of brain-derived neurotrophic factor [J]. *J Neurochem*, 2005, **93**(2): 412-421.
[42] Xiong T, Yang X, Qu Y, *et al*. Erythropoietin induces synaptogenesis and neurite repair after hypoxia ischemia-mediated brain injury in neonatal rats [J]. *Neuroreport*, 2019, **30**(11): 783-789.
[43] Yamada K, Mizuno M, Nabeshima T. Role for brain-derived neurotrophic factor in learning and memory [J]. *Life Sci*, 2002, **70**(7): 735-744.
[44] Lu B, Nagappan G, Lu Y. BDNF and synaptic plasticity, cognitive function, and dysfunction [J]. *Handb Exp Pharmacol*, 2014, **220**: 223-250.
[45] Castren E, Monteggia LM. Brain-derived neurotrophic factor Signaling in Depression and Antidepressant Action [J]. *Biol Psychiatry*, 2021, **90**(2): 128-136.
[46] Colciaghi F, Nobili P, Cipelletti B, *et al*. Targeting PSD95-nNOS interaction by Tat-N-dimer peptide during status epi-

lepticus is neuroprotective in MAM-pilocarpine rat model [J]. *Neuropharmacology*, 2019, **153**: 82-97.
[47] Sen T, Gupta R, Kaiser H, *et al*. Activation of PERK elicits memory impairment through inactivation of CREB and down-regulation of PSD95 after traumatic brain injury [J]. *J Neurosci*, 2017, **37**(24): 5900-5911.
[48] Dore K, Malinow R. Elevated PSD-95 blocks ion-flux independent LTD: a potential new role for PSD-95 in synaptic plasticity [J]. *Neuroscience*, 2021, **456**: 43-49.
[49] Jaroudi W, Garami J, Garrido S, *et al*. Factors underlying cognitive decline in old age and Alzheimer's disease: the role of the hippocampus [J]. *Rev Neurosci*, 2017, **28**(7): 705-714.
[50] Chandrakantan A, Adler AC, Tohsun M, *et al*. Intermittent hypoxia and effects on early learning/memory: exploring the hippocampal cellular effects of pediatric obstructive sleep apnea [J]. *Anesth Analg*, 2021, **133**(1): 93-103.
[51] Li W, Yang S, Yu FY, *et al*. Hydrogen ameliorates chronic intermittent hypoxia-induced neurocognitive impairment *via* inhibiting oxidative stress [J]. *Brain Res Bull*, 2018, **143**: 225-233.
[52] Xu W, Chi L, Row BW, *et al*. Increased oxidative stress is associated with chronic intermittent hypoxia-mediated brain cortical neuronal cell apoptosis in a mouse model of sleep apnea [J]. *Neuroscience*, 2004, **126**(2): 313-23.
[53] Lam CS, Tipoe GL, So KF, *et al*. Neuroprotective mechanism of Lycium barbarum polysaccharides against hippocampal-dependent spatial memory deficits in a rat model of obstructive sleep apnea [J]. *PLoS One*, 2015, **10**(2): e0117990.
[54] Ma Q. Role of nrf2 in oxidative stress and toxicity [J]. *Annu Rev Pharmacol Toxicol*, 2013, **53**: 401-426.
[55] Lian N, Zhang S, Huang J, *et al*. Resveratrol attenuates intermittent hypoxia-induced lung injury by activating the Nrf2/ARE pathway [J]. *Lung*, 2020, **198**(2): 323-331.
[56] Kanninen K, Heikkinen R, Malm T, *et al*. Intrahippocampal injection of a lentiviral vector expressing Nrf2 improves spatial learning in a mouse model of Alzheimer's disease [J]. *Proc Natl Acad Sci U S A*, 2009, **106**(38): 16505-16510.
[57] Bhardwaj M, Deshmukh R, Kaundal M, *et al*. Pharmacological induction of hemeoxygenase-1 activity attenuates intracerebroventricular streptozotocin induced neurocognitive deficit and oxidative stress in rats [J]. *Eur J Pharmacol*, 2016, **772**: 43-50.
[58] Mhillaj E, Catino S, Miceli FM, *et al*. Ferulic acid improves cognitive skills through the activation of the heme oxygenase system in the rat [J]. *Mol Neurobiol*, 2018, **55**(2): 905-916.
[59] Ali T, Kim T, Rehman SU, *et al*. Natural dietary supplementation of anthocyanins *via* PI3K/Akt/Nrf2/HO-1 pathways mitigate oxidative stress, neurodegeneration, and memory impairment in a mouse model of Alzheimer's disease [J]. *Mol Neurobiol*, 2018, **55**(7): 6076-6093.
[60] Zou Y, Hong B, Fan L, *et al*. Protective effect of puerarin against beta-amyloid-induced oxidative stress in neuronal cultures from rat hippocampus: involvement of the GSK-3beta/Nrf2 signaling pathway [J]. *Free Radic Res*, 2013, **47**(1): 55-63.
[61] Lu R, Kiernan MC, Murray A, *et al*. Kidney-brain crosstalk in the acute and chronic setting [J]. *Nat Rev Nephrol*, 2015, **11**(12): 707-719.
[62] Kumral A, Tuzun F, Oner MG, *et al*. Erythropoietin in neonatal brain protection: the past, the present and the future [J]. *Brain Dev*, 2011, **33**(8): 632-643.
[63] Othman M, Rajab E, AlMubarak A, *et al*. Erythropoietin protects against cognitive impairment and hippocampal neurodegeneration in diabetic mice [J]. *Behav Sci (Basel)*, 2018, **9**(1): 4.
[64] Perrone S, Lembo C, Gironi F, *et al*. Erythropoietin as a neuroprotective drug for newborn infants: ten years after the first use [J]. *Antioxidants (Basel)*, 2022, **11**(4): 652.
[65] Nam Y, Joo B, Lee JY, *et al*. ALWPs improve cognitive function and regulate abeta plaque and tau hyperphosphorylation in a mouse model of Alzheimer's disease [J]. *Front Mol Neurosci*, 2019, **12**: 192.
[66] Wei M, Feng S, Zhang L, *et al*. Active fraction combination from Liuwei Dihuang Decoction improves adult hippocampal neurogenesis and neurogenic microenvironment in cranially irradiated mice [J]. *Front Pharmacol*, 2021, **12**: 717719.
[67] Zhang XW, Liu DS, Chen X, *et al*. Liuwei Dihuang Pills combined with Butylphthalide Capsules for the treatment of cerebral small vessel diseases with non-dementia vascular cognitive impairment [J]. *Shanxi Med J*, 2020, **49**(23): 3198-3200.
[68] Zhang RX, Li MX, Jia ZP. Rehmannia glutinosa: review of botany, chemistry and pharmacology [J]. *J Ethnopharmacol*, 2008, **117**(2): 199-214.
[69] Chen H, Deng C, Meng Z, *et al*. Effects of Catalpol on Alzheimer's disease and its mechanisms [J]. *Evid Based Complement Alternat Med*, 2022, **2022**: 2794243.
[70] Dong W, Xian Y, Yuan W, *et al*. Catalpol stimulates VEGF production *via* the JAK2/STAT3 pathway to improve angiogenesis in rats' stroke model [J]. *J Ethnopharmacol*, 2016, **191**: 169-179.
[71] Zhu HF, Wan D, Luo Y, *et al*. Catalpol increases brain angiogenesis and up-regulates VEGF and EPO in the rat after permanent middle cerebral artery occlusion [J]. *Int J Biol Sci*, 2010, **6**(5): 443-453.
[72] Liu F, Lu Z, Li Z, *et al*. Electroacupuncture improves cerebral ischemic injury by enhancing the EPO-JAK2-STAT5 pathway in rats [J]. *Neuropsychiatr Dis Treat*, 2021, **17**: 2489-2498.
[73] Liu J, Narasimhan P, Yu F, *et al*. Neuroprotection by hypoxic preconditioning involves oxidative stress-mediated expression of hypoxia-inducible factor and erythropoietin [J]. *Stroke*, 2005, **36**(6): 1264-9.
[74] Dawson TM. Preconditioning-mediated neuroprotection through erythropoietin? [J]. *Lancet*, 2002, **359**(9301): 96-97.
[75] Bolli R, Dawn B, Xuan YT. Role of the JAK-STAT pathway in protection against myocardial ischemia/reperfusion injury [J]. *Trends Cardiovasc Med*, 2003, **13**(2): 72-79.
[76] Paithankar JG, Saini S, Dwivedi S, *et al*. Heavy metal associated health hazards: an interplay of oxidative stress and signal transduction [J]. *Chemosphere*, 2021, **262**: 128350.
[77] Datta SR, Brunet A, Greenberg ME. Cellular survival: a play in three Akts [J]. *Genes Dev*, 1999, **13**(22): 2905-2927.
[78] Mohi-Ud-Din R, Mir RH, Wani TU, *et al*. Berberine in the treatment of neurodegenerative diseases and nanotechnology enabled targeted delivery [J]. *Comb Chem High Throughput Screen*, 2022, **25**(4): 616-633.
[79] Yang K, Cao F, Xue Y, *et al*. Three classes of antioxidant defense systems and the development of postmenopausal osteoporosis [J]. *Front Physiol*, 2022, **13**: 840293.
[80] Molina-Salinas G, Rivero-Segura NA, Cabrera-Reyes EA, *et al*. Decoding signaling pathways involved in prolactin-induced neuroprotection: A review [J]. *Front Neuroendocrinol*, 2021, **61**: 100913.
[81] Tothova Z, Semelakova M, Solarova Z, *et al*. The role of PI3K/AKT and MAPK signaling pathways in erythropoietin signalization [J]. *Int J Mol Sci*, 2021, **22**(14): 7682.

Cite this article as: SI Jianchao, CHEN Xue, QI Kerong, *et al*. Shengmaisan combined with Liuwei Dihuang Decoction alleviates chronic intermittent hypoxia-induced cognitive impairment by activating the EPO/EPOR/JAK2 signaling pathway [J]. *Chin J Nat Med*, 2024, **22**(5): 426-440.